Computation of conical intersections by using perturbation techniques

Luis Serrano-Andrés[a] and Manuela Merchán[b]
Instituto de Ciencia Molecular, Universitat de València, Dr. Moliner 50, Burjassot, ES-46100 Valencia, Spain

Roland Lindh[c]
Department of Chemical Physics, Lund University, Chemical Center, PO Box 124, SE-22100 Lund, Sweden and Department of Theoretical Chemistry, Lund University, Chemical Center, PO Box 124, SE-22100 Lund, Sweden

(Received 27 October 2004; accepted 12 January 2005; published online 15 March 2005)

Multiconfigurational second-order perturbation theory, both in its single-state multiconfigurational second-order perturbation theory (CASPT2) and multistate (MS-CASPT2) formulations, is used to search for minima on the crossing seams between different potential energy hypersurfaces of electronic states in several molecular systems. The performance of the procedures is tested and discussed, focusing on the problem of the nonorthogonality of the single-state perturbative solutions. In different cases the obtained structures and energy differences are compared with available complete active space self-consistent field and multireference configuration interaction solutions. Calculations on different state crossings in LiF, formaldehyde, the ethene dimer, and the penta-2,4-dieniminium cation illustrate the discussions. Practical procedures to validate the CASPT2 solutions in polyatomic systems are explored, while it is shown that the application of the MS-CASPT2 procedure is not straightforward and requires a careful analysis of the stability of the results with the quality of the reference wave functions, that is, the size of the active space. © *2005 American Institute of Physics*. [DOI: 10.1063/1.1866096]

I. INTRODUCTION

The fundamental role that the crossing seams (or hyperlines) between potential energy surfaces (PES) play in nonadiabatic photochemistry is well recognized by now. The outstanding efforts made by many researchers along the years have provided the foundations, both in the field of methods and applications, in order to locate and characterize such crossings.[1–4] In modern photochemistry the efficiency of radiationless decay between different electronic states taking place in internal conversion and intersystem crossing processes is usually associated to the presence of conical intersections (CI) and crossing hyperplanes which behave as funnels where the probability for nonadiabatic jumps is high.[5,6]

A crossing seam occurs between two states of the same spin multiplicity when they intersect along a $(F-2)$-dimensional hyperline as the energy is plotted against the F nuclear coordinates, where F is the number of internal degrees of freedom $(3N-6)$. In any point of the $(F-2)$-dimensional intersection space the energies of the two states are the same. The degeneracy is lifted along the two remaining linearly independent coordinates, $\mathbf{x_1}$ and $\mathbf{x_2}$, that span the branching subspace corresponding to the gradient difference vector and the nonadiabatic coupling vector, respectively.[5] In order to describe the dynamics of photochemical reactions, full characterization of the hyperline is required. The crossing seam can be viewed as formed by an infinite number of CI points. The denomination *conical intersection* comes from the fact that the corresponding PESs at a CI point have the shape of a double cone when the energy of the upper and lower state is plotted against the $\mathbf{x_1}$ and $\mathbf{x_2}$ coordinates. Normally, in particular for low-energy processes, transition from one state to the other is expected to take place in the region of the lowest-energy point of the hyperline, i.e., at the lowest CI, which is also named minimal in the crossing seam (MXS) (Ref. 7) or minimum energy crossing point.[8] Most of the theoretical efforts have been focused on the localization of the lowest-energy point in the intersection of two PESs.[1,4] Relation between the spatial extension of interaction subspaces and reaction paths is the subject of increasing attention.[9–11]

Determination of CIs have been carried out by using variational wave functions, primarily of the complete active space self-consistent field (CASSCF) (Refs. 12 and 13) and the multireference configuration interaction (MRCI) type, through two main algorithms based on Lagrange multipliers[7,8,14–17] and on projected gradient techniques.[18,19] A typical computational strategy is to perform single-point multiconfigurational second-order perturbation theory (CASPT2) (Refs. 20–22) calculations at CASSCF determined conical intersection geometries, that is, the protocol CASPT2//CASSCF (it also holds true for MRCI//CASSCF). The procedure is only valid when the hypersurfaces described at both levels of theory behave more or less parallel with a constant relative influence of dynamic correlation (hereafter denoted as case A).[23,24] In many situations, because of differential dynamic electron correlation effects which are not accounted for at the CASSCF level, the

[a]Electronic mail: Luis.Serrano@uv.es
[b]Electronic mail: Manuela.Merchan@uv.es
[c]Electronic mail: Roland.Lindh@teokem.lu.se

CASPT2//CASSCF protocol leads to unphysical results (case B) and, therefore, the CI computation has to be performed at a higher level of theory.[25] On the other hand, the use of the accurate MRCI wave functions is restricted to systems of small molecular size.[26] The bottleneck in this approach is imposed by the nature of the MRCI method and it is directly linked to the configuration interaction technology, which undergoes a continuous and outstanding progress.[7]

Despite the great success of the multiconfigurational perturbation theory to describe accurately excited states, with the CASPT2 method being the main protagonist,[27–30] as far as we know there has been only one attempt to directly calculate CIs by using perturbation theory.[31] This strategy might, however, expand the range of applications to include realistic models involving biomolecules. One of the main problems of using perturbation theory to compute PES crossings is that the resulting wave functions corrected up to first order are not, in general, orthogonal. Within the framework of the CASPT2 method, this drawback can be easily overcome by using its multistate extension (MS-CASPT2).[28,32] However, as shall be discussed below, the correct application of the MS-CASPT2 method is not straightforward.

Originally, the idea of the present paper came as a necessity to answer two main questions that arose in the course of our current research in the fields of photochemistry and photobiology by using perturbation theory. First, can the CASPT2 method be confidently applied in a good approximation to locate conical intersections in spite of the nonorthogonality of the resulting wave functions? Second, is the MS-CASPT2 method the general, convenient solution to surmount the nonorthogonality problem? For this purpose a number of cases are considered for which accurate large-scale MRCI results are available for comparison. The paper is organized as follows. Definition of the problem is considered in the following section, together with the methodological key points. Four examples of crossings between states are then explored. Initially, an avoided crossing in a diatomic system, LiF, is analyzed, to continue with three more examples of conical intersections involving the molecular systems: formaldehyde, ethene dimer, and the penta-2,4-dieniminium cation, a simple model for the retinal protonated Schiff base.

II. DEFINITION OF THE PROBLEM AND METHODOLOGICAL DETAILS

The CASPT2 method[20–22] is a conventional nondegenerate second-order perturbation theory in which a single-reference function is considered, with the particularity that such zeroth-order reference function is a CASSCF wave function and uses internal contraction in its formulation. The *multistate* CASPT2 procedure[28,32,33] represents an extension of the CASPT2 method for the perturbation treatment of chemical situations that require two or more reference states. For instance, the proper description of situations such as avoided crossings and near degeneracy of valence and Rydberg states cannot, in general, be fully accounted for by just using a single-reference perturbation treatment.

In the MS-CASPT2 method[24,33] an effective Hamiltonian matrix is built where the diagonal elements are the CASPT2 energies and the off-diagonal elements take into account the coupling up to second order of dynamic correlation energy. Starting from a set of N orthogonal average CASSCF wave functions Φ_i $(i=1,N)$, for which average molecular orbitals are available, N single-state CASPT2 calculations are performed. In order to build the matrix representation of the Hamiltonian using as basis set the N normalized wave functions corrected up to first order, $\Psi_i=\Phi_i+\Psi_i^{(1)}$, the following matrices are defined:

$$S_{ij}=\langle\Psi_i|\Psi_j\rangle=\langle\Phi_i+\Psi_i^{(1)}|\Phi_j+\Psi_j^{(1)}\rangle=\delta_{ij}+s_{ij}, \tag{1}$$

$$\langle\Phi_i|\hat{\mathrm{H}}|\Phi_j\rangle=\delta_{ij}E_i, \tag{2}$$

$$\langle\Phi_i|\hat{\mathrm{H}}|\Psi_j^{(1)}\rangle=e_{ij}. \tag{3}$$

Notice that the two wave functions are not orthogonal, since $\langle\Phi_i|\Phi_j\rangle=\delta_{ij}$ and $\langle\Phi_i|\Psi_j^{(1)}\rangle=0$, but $\langle\Psi_i^{(1)}|\Psi_j^{(1)}\rangle=s_{ij}$. On the other hand, the CASSCF energy for state i is represented by E_i and the elements e_{ij} are the CASPT2 correlation energies. For each state, the Hamiltonian can be expressed as the sum of a zeroth-order contribution and a Hamiltonian taking care of the remaining effects

$$\hat{\mathrm{H}}=\hat{\mathrm{H}}_i^0+\hat{\mathrm{H}}_i'. \tag{4}$$

Therefore, the following equations are fulfilled up to second order:

$$\langle\Psi_i^{(1)}|\hat{\mathrm{H}}|\Psi_j^{(1)}\rangle\approx\langle\Psi_i^{(1)}|\hat{\mathrm{H}}_i^0|\Psi_j^{(1)}\rangle\approx\langle\Psi_i^{(1)}|\hat{\mathrm{H}}_j^0|\Psi_j^{(1)}\rangle. \tag{5}$$

The elements $\langle\Psi_i^{(1)}|\hat{\mathrm{H}}_i'|\Psi_j^{(1)}\rangle$ correspond to a third-order correction and, consequently, they are not considered. The matrix representation of the Hamiltonian is not symmetric $H_{12}\neq H_{21}$. Assuming that the off-diagonal terms are very similar, as it is implicit from Eq. (5), the matrix is made symmetric by using the average value

$$\langle\Psi_i^{(1)}|\hat{\mathrm{H}}|\Psi_j^{(1)}\rangle=\tfrac{1}{2}(\langle\Psi_i^{(1)}|\hat{\mathrm{H}}_i^0|\Psi_j^{(1)}\rangle+\langle\Psi_i^{(1)}|\hat{\mathrm{H}}_j^0|\Psi_j^{(1)}\rangle). \tag{6}$$

The matrix element including zeroth-, first-, and second-order corrections takes the general form

$$\hat{\mathrm{H}}_{ij}=\langle\Psi_i|\hat{\mathrm{H}}|\Psi_j\rangle=\delta_{ij}\mathrm{E}_i+\tfrac{1}{2}(e_{ij}+e_{ji})+\tfrac{1}{2}(E_i^{(0)}+E_j^{(0)})S_{ij}. \tag{7}$$

By solving the corresponding secular equation $(\mathbf{H}-E\mathbf{S})\mathbf{C}=0$, the eigenfunctions and eigenvalues can be obtained. They correspond to the MS-CASPT2 wave functions and energies, respectively.

The MS-CASPT2 wave function can be finally written as

$$\Psi_p=\sum_i C_{pi}|i\rangle+\Psi_p^{(1)}=|i_p\rangle+\Psi_p^{(1)}, \tag{8}$$

where $|i\rangle$ are the CASSCF reference functions and $\Psi_p^{(1)}$ is the first-order wave function for state p. Accordingly, the function $|i_p\rangle$, formed by a linear combination of the CAS states involved in the MS-CASPT2 calculation, is the model state and can be considered as a new reference function for state p. The reference functions $|i_p\rangle$ are the so-called *perturbation*

modified CAS.[32] They are used for the computation of transition properties and expectation values at the MS-CASPT2 level.

For the proper use of the MS-CASPT2 method, condition (5) has to be fulfilled. It means in practice that the asymmetric effective Hamiltonian matrix should have small and similar off-diagonal elements. Otherwise, the average process carried out, $(H_{12}+H_{21})/2$, may lead to unphysical results, in both the MS-CASPT2 energies and eigenfunctions. The condition $H_{12}\cong H_{21}$ can be achieved by enlarging the active space, which implies a redefinition of the zeroth-order Hamiltonian. Large active spaces, beyond the main valence MOs, are used naturally in the simultaneous treatment of valence and Rydberg states, where the MS-CASPT2 approach has proved to be extremely useful.[32,34,35] Special caution has to be exercised, however, for the computation of a crossing point between two surfaces, as in the case of conical intersections (and avoided crossings), crucial in photochemistry.

The states involved in a conical intersection have usually different nature. Quite often one state has covalent character, whereas the other is zwitterionic. They are described by hole-hole and hole-pair VB structure, respectively. The effect of dynamic electron correlation is usually much more pronounced for zwitterionic than for covalent states. As a result, with moderate (valence) active spaces, the off-diagonal elements become very different, because the covalent state is described comparatively better than the zwitterionic state. Active spaces comprising molecular orbitals (MOs) beyond the valence shell would be required to make $H_{12}\cong H_{21}$. In addition, the structure of the 2×2 effective Hamiltonian is

$$H^{\text{eff}}=\begin{pmatrix} H_{11} & H_{12} \\ H_{21} & H_{22} \end{pmatrix} \approx \begin{pmatrix} E_1^{\text{PT2}} & \Delta \\ \Delta & E_2^{\text{PT2}} \end{pmatrix}, \tag{9}$$

where $E_1^{\text{PT2}}=E_1+e_{11}$ and $E_2^{\text{PT2}}=E_2+e_{22}$ are the CASPT2 energies of the two states and $\Delta=(H_{12}+H_{21})/2$. If the states become degenerate at the CASPT2 level, $E_1^{\text{PT2}}=E_2^{\text{PT2}}=E$, the multistate energies and wave functions are

$$E_{\pm}=E\pm\Delta, \tag{10}$$

$$\Psi_{\pm}=\frac{1}{\sqrt{2}}(\Psi_1\pm\Psi_2). \tag{11}$$

As $\Delta=0$ the MS-CASPT2 and the CASPT2 solutions are equivalent, what is expected to occur at a conical intersection. Therefore, by providing enough flexibility to the active space, one has to make sure that the condition $H_{12}\cong H_{21}$ is satisfied and $\Delta\leqslant 2$ kcal/mol. As a conclusion, computation of surface crossings at the CASPT2 and MS-CASPT2 level is expected to require more extended active spaces than those used at the CASSCF level. What happens if Δ is larger than 2 kcal/mol? For systems of relatively large molecular size one cannot be sure whether that result points out to the presence of an avoided crossing or it is just spurious because of the limited active space employed. Additionally, dynamic correlation plays sometimes a crucial role in determining the nature of the lowest surface crossings.[24,25] In this respect, recent advances on analytic energy gradients for general MRPT methods seem very promising.[36]

In the present work we attempt to find practical procedures to analyze the accuracy of the results obtained in the crossing regions at the CASPT2 and MS-CASPT2 levels. Methodological efforts are however certainly required to improve the present methodology. All calculations have been performed using a modified version of the MOLCAS-6 code.[37–39] Searching of conical intersections at both the CASSCF and CASPT2 levels (using analytical and numerical gradients for the two methods, respectively) employ an algorithm based on a modified version of the method suggested by Anglada and Bofill[17] to use a Lagrange multiplier optimization scheme, in conjunction with a internal coordinates space division into a constraint subspace and a reduced subspace in which the optimization is performed. Work is in progress to introduce at the different levels the calculation of nonadiabatic coupling elements, which are not considered here.

III. RESULTS AND DISCUSSION

A. LiF

The ionic-neutral potential curve crossings involving the ground and low-lying excited states of alkaline halide compounds has been repeatedly studied in order to find good representations of the adiabatic potentials and the nonadiabatic coupling matrix elements (NACMEs) consequence of the breakdown of the Born–Oppenheimer approximation. In LiF, the ground $X\,^1\Sigma^+$ state at short internuclear bond distances is basically described by the ionic $|1\sigma^2 2\sigma^2 3\sigma^2 4\sigma^2 1\pi^4\rangle$ configuration state function (CSF), while the nearby excited $A\,^1\Sigma^+$ state can be better characterized by the neutral $|1\sigma^2 2\sigma^2 3\sigma^2 4\sigma^1 5\sigma^1 1\pi^4\rangle$ CSF. Considering that the dissociation limit leading to the ionic atoms is higher than the corresponding neutral channel, both states undergo an avoided crossing upon increasing the bond distance because of the noncrossing rule that applies for states of the same symmetry in diatomic systems. On interaction, along the potential energy curves, the character of the wave functions changes gradually, and after the crossing, that is, at long internuclear distances, the ground state becomes neutral and the excited state ionic. In order to describe the change in the curve properties smoothly, a flexible and accurate method is required. It was shown that a state-average (SA) CASSCF procedure combined with the MRCI method was an adequate level to treat the problem and approach the full-CI solution.[40] Once the adiabatic potentials are obtained, further procedures can be used to compute the NACMEs in a proper way.[40]

Instead of using a MRCI approach one may try to employ a less expensive procedure such as a second-order multiconfigurational method, CASPT2. It was already pointed out[41] that the CASPT2 curves in LiF erroneously cross at two different points along the dissociation distance. Indeed, the obtained CASPT2 solutions are based on a single CASSCF reference and they are not necessarily orthogonal. The selection of the basis sets and, especially, the active space will have dramatic consequences in the description of the crossing. The MS-CASPT2 method has been claimed[32,42]

as an accurate procedure to describe adiabatic potential energy curves in crossing regions. As described above the multistate approach yields an orthogonalization of the interacting CASPT2 states. The larger is the coupling of the reference states, the larger will be the splitting of the adiabatic curves. In the present research we have performed a systematic study of the avoided crossing between the low-lying $^1\Sigma^+$ states of LiF using the CASPT2 and MS-CASPT2 approach. Our goal is just to illustrate the behavior of the methods in the calculation of state crossings. Complementary studies using larger basis sets can be found[40,42] where computed spectroscopic parameters are compared to experiment. The present calculations employed an atomic natural orbital basis set[43] formed by Li[4*s*2*p*]/F[4*s*3*p*1*d*] contracted functions. Several active spaces were used. Only three of them will be shown here for the sake of brevity. The minimal active space required to described correctly the dissociation process includes two σ orbitals ($4\sigma 5\sigma$), one π orbital (1π), and six electrons, an space that we will coin (2,1). The 1σ-3σ MOs were treated as inactive and the core orbitals were not correlated at the second-order level. Figure 1 displays the potential energy curves for the ground $X\ ^1\Sigma^+$ and excited $A\ ^1\Sigma^+$ states of LiF in the range of internuclear distances 6–15 a.u. computed at the CASPT2 and MS-CASPT2 levels. The results are based on a SA-CASSCF reference including the two states of interest. The CASPT2(2,1) states [Fig. 1(a)] are clearly nonorthogonal, violate the noncrossing rule, and their adiabatic curves have two crossing points near 8.4 and 9.8 a.u. On the contrary, the MS-CASPT2 curves seem to exhibit the proper behavior in the avoided crossing region, although the splitting is clearly too large. The best MRCI estimate for the vertical splitting between the two uncorrected adiabatic curves is nearly 1.5 kcal/mol close to 12.6 a.u. (see Fig. 7 in Ref. 40), while the minimal MS-CASPT2(2,1) splitting is 6.9 kcal/mol at 10.4 a.u.

More accurate results can be certainly obtained by improving the reference states through the enlargement of the active space. One has to bear in mind that the purpose of the present contribution is to analyze if the states crossings can be accurately computed by perturbation theory. In describing the LiF ionic-neutral crossing, the CASPT2 curves should not cross, while the MS-CASPT2 curves should not yield too large and unphysical splittings. The active space can be extended in different ways. Increasing the number of σ orbitals permits a better description of the radial correlation effects of the halogen *np* electrons, which turned out to be of minor importance in the present case. It was not until the angular correlation effects were taken into account by enlarging the π space that the CASPT2 curves avoided the crossing. Results employing two additional active spaces are also included in Fig. 1: six active electrons in (4,3) and (4,4) active orbitals. The CASPT2(4,3) curves nearly avoid the crossing, while in the latter case both descriptions, CASPT2(4,4) and MS-CASPT2(4,4), are equivalent. The CASPT2(4,4)/MS-CASPT2(4,4) minimal vertical splitting between the two curves at 11.8 a.u. is 2.3 kcal/mol, much closer to the MRCI result (obtained with a larger basis set). Which is the basic conclusion we can obtain from these results? Certainly, an accurate description of states crossings cannot be obtained by using CASPT2 unless the states become practically orthogonal. It is possible however to check this aspect by performing a subsequent MS-CASPT2 treatment, which provides purely orthogonal solutions that can be compared with the CASPT2 findings. When both, CASPT2 and MS-CASPT2 methods yield the same solutions we can be certain about the reliability of the results within a given level of calculation. Why not to use directly the orthogonal MS-CASPT2 states? As it has been shown in this example, the

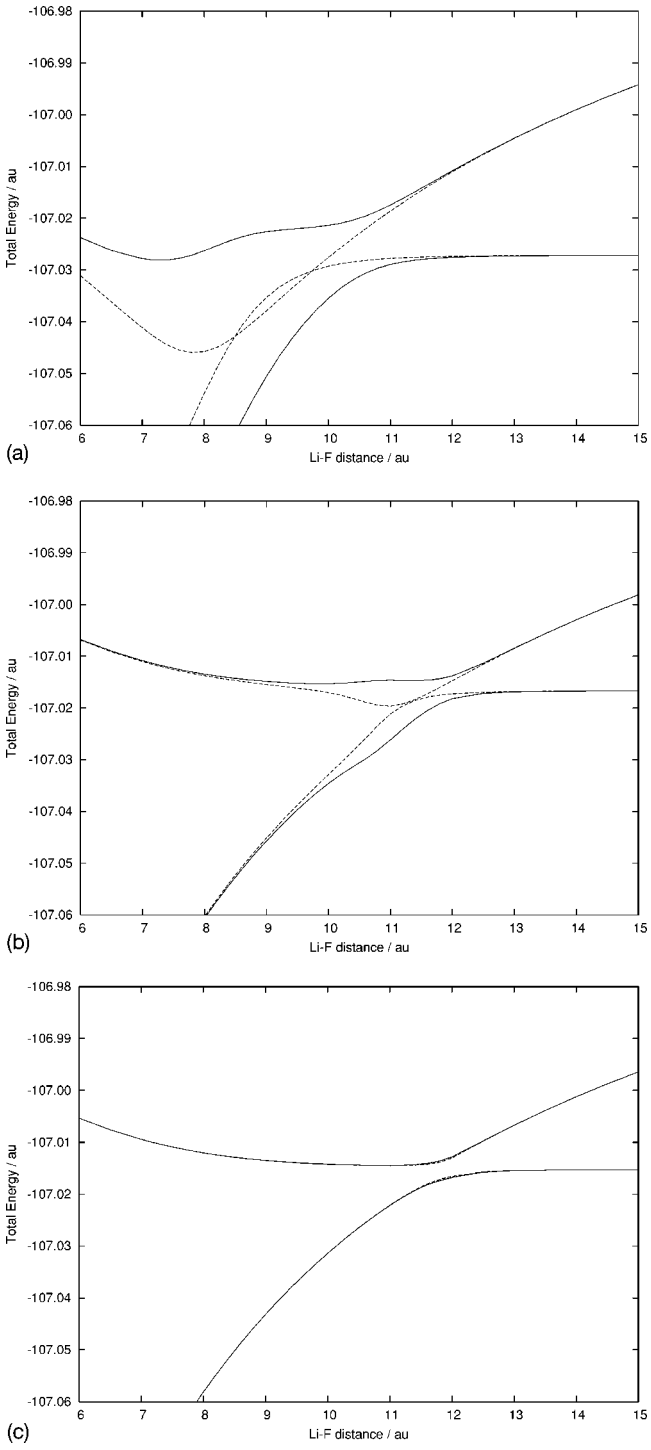

FIG. 1. CASPT2 (dotted lines) and MS-CASPT2 (full lines) potential energy curves describing the crossing of the $^1\Sigma^+$ states of LiF along the internuclear distance. From top to bottom the employed active spaces included six electrons and (a) (21), (b) (43), and (c) (44) C_{2v} orbitals, respectively.

TABLE I. Computed geometries and energies for the ground state and the MXS point for the $1\,^1B_1/2\,^1A_1$ states of formaldehyde at different levels of theory.

	R_{CO}(Å)	R_{CH}(Å)	$\angle CH_2$(°)	E(a.u.)	ΔE(eV)
			cc-pVDZ		
CASSCF					
GS($1\,^1A_1$)[a]	1.220	1.097	116.9	−113.950 044	0.00 (0.00)[b]
	(1.224)[b]	(1.095)[b]	(117.7)[b]	(−113.928 787)[b]	
MXS($1\,^1B_1/2\,^1A_1$)[c]	1.586	1.078	130.9	−113.614 162	9.14 (8.56)[b]
MRCI(SD)[c]					
GS($1\,^1A_1$)	1.218	1.112	115.7	−114.200 952	0.00
MXS($1\,^1B_1/2\,^1A_1$)	1.549	1.097	123.5	−113.893 023	8.38
CASPT2					
GS($1\,^1A_1$)	1.216	1.113	115.6	−114.189 923	0.00
MXS($1\,^1B_1/2\,^1A_1$)	1.530	1.096	124.4	−113.886 504	8.26
MS-CASPT2					
GS($1\,^1A_1$)	1.216	1.113	115.6	−114.189 923	0.00
MXS($1\,^1B_1/2\,^1A_1$)	1.530	1.096	124.4	−113.886 504	8.26
			cc-pVTZ		
CASSCF					
GS($1\,^1A_1$)[a]	1.215	1.088	117.2	−113.985 284	0.00 (0.00)[b]
	(1.220)[b]	(1.086)[b]	(118.0)[b]	(−113.961 690)[b]	
MXS($1\,^1B_1/2\,^1A_1$)[c]	1.570	1.067	132.7	−113.652 840	9.05 (8.40)[b]
MRCI(SD)[c]					
GS($1\,^1A_1$)	1.212	1.095	116.7	−114.305 460	0.00
MXS($1\,^1B_1/2\,^1A_1$)	1.529	1.078	132.7	−114.004 987	8.18
CASPT2					
GS($1\,^1A_1$)	1.210	1.098	116.5	−114.302 546	0.00
MXS($1\,^1B_1/2\,^1A_1$)	1.513	1.084	126.2	−114.009 131	7.98
MS-CASPT2					
GS($1\,^1A_1$)	1.210	1.098	116.5	−114.302 546	0.00
MXS($1\,^1B_1/2\,^1A_1$)	1.513	1.084	126.2	−114.009 131	7.98

[a]Ground state optimized as the first root of a single-root CASSCF calculation.
[b]Ground state optimized as the first root of a three-root SA-CASSCF calculation. Reference 38.
[c]Results from Ref. 38.

orthogonalization procedure will not be accurate unless the reference states are good enough. Unfortunately, to reach orthogonality of the wave functions corrected up to first order (like in CASPT2) is a difficult task because it implies enlarging the active space further from the practical possibilities quite often. The convergence of the results with respect to the active space becomes more difficult as larger is the basis sets employed, because, in order to provide accurate results, comparatively larger active spaces are then required. We will try to find some useful procedure in the following examples.

B. Formaldehyde

Formaldehyde (H_2CO) has an intersection between the hypersurfaces of the $2\,^1A_1(\pi\pi^*)$ and $1\,^1B_1(\sigma\pi^*)$ excited states at C_{2v} symmetry. Recently, Lischka *et al.*[7,44] have reported results on the system at the MRCI level. Table I compiles calculations on the lowest-energy intersection point of formaldehyde at the CASSCF, CASPT2, and MS-CASPT2 levels of theory, as well as the previous MRCI results. The employed active space included six electrons and the $\sigma(5a_1)$, $\pi(1b_1)$, $n(2b_2)$, $\pi^*(2b_1)$, and $\sigma^*(6a_1)$ orbitals. The state-average CASSCF procedure included three states, $1\,^1A_1$, $2\,^1A_1$, and $1\,^1B_1$. Although the calculations were performed within the C_s point group, with the symmetry plane perpendicular to the molecular plane, and no further symmetry restrictions were imposed, the wave functions kept C_{2v} symmetry. Two basis sets, cc-pVDZ and cc-pVTZ (Ref. 45) were employed in order to compare with the previous MRCI calculations.

The results reported in Table I show that the ground state optimizations are basically equivalent at the MRCI and CASPT2 levels of theory. Regarding the optimization of the MXS point, the main geometric changes taking place with respect to the ground state include the elongation of the CO and CH bond distances by near 0.3 and 0.015 Å, respectively, and the increasing of the CH_2 angle by 8–12°. Again, MRCI and CASPT2 lead to quite similar descriptions. The only significant difference between both methods occurs in the CO bond length. The perturbative treatment leads to an estimated bond distance 0.019 Å (cc-pVDZ) and 0.016 Å (cc-pVTZ) shorter than the MRCI optimization. The sensitivity of the optimized CO bond distance with respect to the level of theory is well known. The small discrepancies found between MRCI and CASPT2 have to be related to the intrinsic differences in the two methodologies. Another important issue relates to the orthogonality of the CASPT2 solutions. As displayed in Table I, the CASPT2 and MS-CASPT2 results are equivalent. Considering that the computed states,

TABLE II. Computed geometries and energies for the MXS point of the $1\,^1A_g(G)/2\,^1A_g(S)$ states in the C_{2h} ethylene dimer at different levels of theory. Basis set: cc-pVDZ; active space $(0202,4e^-)$. Distances R in Angstroms and angles ($\angle$,op=out-of-plane) in degrees.

Method	$R_{c=c}$	R_{c-c}	$\angle$CCC	$R_{CH(1)}$	$R_{CH(2)}$	$\angle CH_{2(1)}$	$\angle CH_{2(2)}$	$opCH_{2(1)}$	$opCH_{2(2)}$	$E+155$ (a.u.)	ΔE (eV)
						Ground state. Separated systems					
CASSCF[a]	1.345	⋯	⋯	1.083	1.083	117.0	117.0	0.0	0.0	−1.126 815	0.00
MRCI(SD)[a]	1.346	⋯	⋯	1.090	1.090	116.3	116.3	0.0	0.0	−1.616 964	0.00
CASPT2[b]	1.349	⋯	⋯	1.094	1.094	117.1	117.1	0.0	0.0	−1.645 522	0.00
						MXS ethylene dimer					
CASSCF[b]	1.443	2.181	109.2	1.081	1.082	114.5	117.5	28.5	23.4	−0.956 643	4.63
MRCI(SD)[a]	1.442	2.166	108.1	1.088	1.087	114.8	117.8	22.6	18.9	−1.462 809	4.19
CASPT2[b]	1.449	2.188	107.0	1.094	1.094	115.6	118.0	24.4	21.1	−1.506 894	3.77

[a]Ground state optimized from a three-root SA-CASSCF calculation. Reference 38.
[b]Optimized from a two-root SA-CASSCF calculation.

$2\,^1A_1$ and $1\,^1B_1$ belong to two different symmetries in the C_{2v} group and that the symmetry of the states is not broken, the CASPT2 solutions are orthogonal and therefore they can be directly used to compute the crossing points. The same behavior will be obtained between states of different multiplicities, for instance to compute singlet-triplet crossing hyperplanes. On the other hand, it is worth mentioning that truncated configuration interaction treatments tend to underestimate correlation energy effects on excited states and provide too high excitation energies (even several eV), especially when the size of the system starts to grow.[46]

Ethene dimer

MRCI results on conical intersections are also available for the photocyclodimerization of two ethylene molecules.[44] Considering the four π,π^* orbital space of the two separated ethylene units, the dimer presents three low-lying states: the ground state, with a configuration $1\pi^2 2\pi^2$, a singly excited state with a configuration $1\pi^2 2\pi^1 3\pi^1$, and a doubly excited state with a configuration $1\pi^2 3\pi^2$. At rectangular configurations two crossings of the single and double excited states are predicted.[44] Instead, we will focus here in the crossing that takes place in the parallelogram structure (C_{2h} symmetry) between the ground $1\,^1A_g$ and the singly excited $2\,^1A_g$ states, comparing the perturbative and the variational MRCI results.[44] The present CASSCF and CASPT2 optimizations were carried out using a cc-pVDZ basis set[45] and including an active space of four electrons and four π orbitals, the same conditions as the MRCI calculations. The C_{2h} symmetry was actually employed, with z as the C_2 axis, the four carbon atoms in the XY plane, and axis y as the distance of approach of the two ethylene moieties. The active space is labeled within the C_{2h} symmetry, ($a_g b_g b_u a_u$, active e^-). Two and three states (including additionally the doubly excited state) were used in the state averaging procedure (SA-CASSCF), although finally only the two-state results will be reported in Tables II and III because no significant differences were found between the two treatments. One has to make sure that the proper wave functions (ground and singly excited states) are obtained all along the optimization procedure.

Table II compiles the previous and the present results. The energy and structure of the separated system of two ethylene moieties computed as a supermolecule has also been included. There is a general agreement between the three treatments [CASSCF, MRCI(SD) and CASPT2], except for the CH bond length obtained at the CASSCF level. At the optimized MXS point the length of the ethylene C–C bond enlarges by 0.1 Å. The computed distance at the MRCI level, 1.442 Å, is 0.018 Å shorter than that obtained by CASPT2. Regarding the interethylene C–C bond distances, the MRCI produces a value shorter by 0.022 Å with respect to CASPT2. For the remaining geometric parameters, including the out-of-plane angles, the agreement between the MRCI and CASPT2 treatments is reasonable. Unlike the example of formaldehyde, here the crossing is computed between states of the same symmetry, therefore the CASPT2 solutions are not formally orthogonal. In addition, the CASPT2 MXS optimization performed here does not contain the estimation of the NACMEs which may have influence in the position of the crossing seam and on the minimal-energy conical intersection within the hyperline. In this sense, the MRCI result for formaldehyde can be considered more accurate. Considering that the computed CASSCF MXS points

TABLE III. Computed MS-CASPT2 energies and off-diagonal Hamiltonian matrix elements for the MXS point of the $1\,^1A_g(G)/2\,^1A_g(S)$ states in the C_{2h} ethylene dimer. The MS-CASPT2 calculations comprise two roots at the CASPT2$(2020,4e^-)$ optimized $1\,^1A_g(G)/2\,^1A_g(S)$ MXS geometry.

Active spaces	E_1+156 (a.u.) CASPT2 $1\,^1A_g$	E_2+156 (a.u.) CASPT2 $2\,^1A_g$	ΔE_{CASPT2} (kcal/mol)	$-H_{12}$ (kcal/mol)	$-H_{21}$ (kcal/mol)	$-(H_{12}+H_{21})/2$ (kcal/mol)	E_1+156 (a.u.) MS-CASPT2 $1\,^1A_g$	E_2+156 (a.u.) MS-CASPT2 $2\,^1A_g$	$\Delta E_{MS\text{-}CASPT2}$ (kcal/mol)
$2020,4e^-$	−0.506 894	−0.506 246	0.41	1.96	2.44	2.20	−0.510 051	−0.502 990	4.42
$3030,4e^-$	−0.506 588	−0.503 276	2.08	2.09	2.89	2.49	−0.509 232	−0.500 632	5.40
$4040,4e^-$	−0.506 527	−0.501 192	3.35	2.60	5.12	3.86	−0.510 565	−0.497 154	8.41
$4040,8e^-$	−0.507 924	−0.503 507	2.76	2.51	5.48	4.00	−0.512 457	−0.498 975	8.46
$4242,12e^-$	−0.514 089	−0.517 478	2.13	1.27	0.03	0.65	−0.517 771	−0.513 796	2.49

TABLE IV. Energy difference between S_1 and S_0, ΔE, computed at the optimized structures of the penta-2,4-dieniminium cation S_1/S_0 conical intersection at different levels. The 6-31G(d) basis set was used throughout. The off-diagonal elements of the MS-CASPT2 effective Hamiltonian H^{eff} are also included. Geom. I: S_1/S_0 CI optimized at the CASSCF(6MOs/6e) level from Ref. 41.

Method	Geom. I (6MOs/6e)	Geom. I (8MOs/6e)	Geom. II[a] (6MOs/6e)	Geom. II[a] (8MOs/6e)	Geom. III[b] (8MOs/6e)	Geom. III[b] (14MOs/6e)	Geom. IV[c] (8MOs/6e)	Geom. IV[c] (14MOs/6e)
				$\Delta E(S_1\text{-}S_0)$ (kcal/mol)				
CASSCF	0.07	4.78	3.40	8.26	0.33	5.23	4.39	8.32
CASPT2	0.99	0.60	3.83	2.30	4.05	1.98	0.62	0.99
MS-CASPT2	7.57	0.64	3.89	2.31	4.27	1.99	8.52	2.92
				Off-diagonal elements of the H^{eff} (kcal/mol)				
H_{12} (asymmetric)	6.12	0.18	0.62	0.14	1.30	0.19	6.91	3.19
H_{21} (asymmetric)	1.38	0.04	0.09	0.01	0.05	0.02	1.59	0.44
$H_{12}=H_{21}$ (symmetric)	3.75	0.11	0.35	0.08	0.67	0.08	4.25	1.37

[a]Geom. II: S_1/S_0 MXS optimized at the CASPT2(6MOs/6e) level.
[b]Geom. III: S_1/S_0 MXS optimized at the CASSCF(8MOs/6e) level.
[c]Geom. IV: S_1/S_0 MXS optimized at the CASPT2(8MOs/6e) level.

led to the same structures both employing NACMEs or not, this effect is not crucial in the present example.

As discussed in previous sections, there are two procedures to obtain orthogonal or quasiorthogonal solutions based on truncated perturbative treatments. Thus, orthogonal solutions can be reached either by enlarging the active space or by applying the MS-CASPT2 correction. In Table III we have combined both ways in order to check the quality of the obtained CASPT2 crossing point. At the optimized CASPT2(2020,4e^-) level, the energy difference between both states is 0.41 kcal/mol. Applying the MS-CASPT2 approach the states energy difference increases to 4.42 kcal/mol. The average off-diagonal Hamiltonian MS-CASPT2 element Δ is computed to be 2.20 kcal/mol. Since the states are nearly degenerate at the CASPT2 level, the MS-CASPT2 splitting amounts to almost 2Δ. Considering these results, one may think that the optimized CASPT2 geometry for the crossing is not correct because the states are clearly nonorthogonal. The results can be however validated at higher level of calculation if we increase the active space at the same geometry and compare the obtained CASPT2 and MS-CASPT2 results. As observed in Table III the increasing of the reference space may not be straightforward. While just the π space was increased no improvement in the treatment was observed. On enlarging the space, obviously, the CASPT2 energy difference was increasing (the geometry was strictly optimized for the smallest active space), but also the MS-CASPT2 splitting. The off-diagonal Hamiltonian elements do not change in that case, meaning that the coupling between the states is retained. The MS-CASPT2 splitting is then larger than 2Δ. It is finally when the σ-π correlation is considered (active space 4242,12e^-) that the reference largely improves. This is reflected not in the CASPT2 splitting (2.13 kcal/mol), but in the magnitude of the off-diagonal elements, which represents the extent of the state coupling. Δ becomes 0.65 kcal/mol, and the splitting between the CASPT2 and MS-CASPT2 energy differences is less than 0.4 kcal/mol. In practice, at that level we can consider both solutions, CASPT2 and MS-CASPT2, equivalent, and therefore the CASPT2 states are nearly orthogonal. It is up to us to establish a criterion to determine if the energy differences at the CASPT2 optimized geometry, 2.13 kcal/mol (CASPT2) and 2.49 kcal/mol (MS-CASPT2), are small enough to consider that point to be a conical intersection or a weakly avoided crossing. In order to validate the CASPT2 results to compute state crossings we suggest to establish the rule that when the difference between the CASPT2 and MS-CASPT2 energy difference is smaller than the splitting expected in conical intersections (nearly 2 kcal/mol), the CASPT2 results can be considered accurate enough. A new illustration of this point will be presented in the following section.

D. The penta-2,4-dieniminium cation

De Vico *et al.*[47] reported the optimized structures for the S_1/S_0 conical intersection along the *cis-trans* isomerization path in the penta-2,4-dieniminium cation (CH_2–C_aH–C_bH–C_cH–C_dH–NH_2^+), a model for the retinal protonated Schiff base. The conical intersections were computed at the CASSCF(6MOs/6e^-) and CASPT2(6MOs/6e^-) levels, hereafter denoted as Geom. I and Geom. II, respectively. Our goal is to establish the behavior of the CASPT2 approach in this case, and here we complement the optimizations by obtaining the MXS points at the CASSCF (8MOs/6e^-), Geom. III, and CASPT2(8MOs/6e^-), Geom. IV, levels. Table IV shows the CASSCF, CASPT2, and MS-CASPT2 energy differences ΔE between S_1 and S_0 computed at those geometries using different active spaces. The 6-31G(d) basis set was used throughout. When the energy difference is less than 2 kcal/mol, the minimum reached is considered technically as a conical intersection; otherwise ($\Delta E \geqslant 2$ kcal/mol) we are facing an avoided crossing. The structural differences between the four geometries are minimal. Bond lengths differ by less than 0.01 Å, and the main geometrical distortion leading to the conical intersection, the change in the dihedral angle of the polyene ($C_aC_bC_cC_d$), reaches in all cases a nearly perpendicular conformation: $-92.2°$ (Geom. I and II), $-90.0°$ (Geom. III), and $-89.7°$ (Geom. IV). The obtained structures all belong to the vicinities of the conical intersection.

Employing Geom. I, the states are degenerated at the

CASSCF level (0.07 kcal/mol) at which the optimization was performed. The CASPT2(6/6) treatment yields an energy difference of 0.99 kcal/mol. It indicates that the optimal geometry determined for the conical intersection at both levels of theory is probably very similar. Prior to establish that the geometry corresponds to a true CASPT2 conical intersection (within the limitations already mentioned regarding the calculation of NACMEs) one has to analyze the effect of orthogonality. The states are separated by 7.57 kcal/mol when they are allowed to interact at the MS-CASPT2 level. As can be seen in Table IV, the off-diagonal elements of H^{eff} are very different, 6.12 and 1.38 kcal/mol. Because the states are nearly degenerate at the CASPT2 level, the result for the off-diagonal symmetric H^{eff} just comes out from averaging: $\Delta=(6.12+1.38)/2$. As a consequence, the CASPT2 states are pushed down and up by the amount 3.75 kcal/mol. Such interaction is definitely unphysical. Enlarging the active space with two extra orbitals (8MOs/6*e* results), which allows for radial correlation of the electrons involved in the 90°-twisted double bond, the H_{12} and H_{21} asymmetric elements become small enough, which reflects that the corresponding zeroth-order Hamiltonians are capable of yielding a balanced description for both states. Accordingly, the CASPT2(8/6) and MS-CASPT2(8/6) splitting between the S_1 and S_0 states becomes small (certainly smaller than 2 kcal/mol). In summary, the computed geometry at the CASSCF (6MOS/6*e*) represents also a conical intersection at the CASPT2(8/6)/MS-CASPT2(8/6) level and it can be validated as a proper result for the crossing.

At Geom. II the MS-CASPT2(6/6) result is 3.89 kcal/mol, similar to the CASPT2(6/6) finding (3.83 kcal/mol), and the off-diagonal matrix elements of the asymmetric effective Hamiltonian H^{eff} are small (less than 2 kcal/mol). Everything seems to be quite consistent. Increasing the active space to (8/6) nothing really changes. Both the CASPT2 (8/6) and MS-CASPT2(8/6) energy differences remain similar and larger than 2 kcal/mol. Considering that the energy differences in Geom. I are much lower than the criterion typically used to determine conical intersections, we may regard Geom. I as a conical intersection point within the crossing seam. Apparently an avoided crossing has been really found when optimizing at the CASPT2(6/6) level, Geom. II. When the optimizations are performed using the larger active space, Geom. III (CASSCF) and Geom. IV (CASPT2), the opposite results are obtained. While the CASSCF(8/6) geometry seems to belong to an avoided crossing region, the CASPT2(8/6) geometry apparently corresponds to a conical intersection point in the crossing seam. To validate the obtained CASPT2(8/6) result we have to enlarge the active space, (14MOs/6e^-), including a much improved reference. Smaller spaces did not reduce the CASPT2/MS-CASPT2 gap up to the required levels (2 kcal/mol). It is clear, the smaller is the obtained CASPT2 energy difference (0.62 kcal/mol at Geom. III), the higher are the orthogonality requirements, and the active space has to be enlarged much more. Therefore, Geom. I and IV correspond to different points of the crossing seam. The latter can be considered the minimum energy crossing point because it has a lower absolute energy for the excited state at the CASPT2 (8/6) level of theory.

In the present example the differences in the obtained geometries at levels as different as CASSCF and CASPT2 are really of minor extent. This is not a surprise because this type of conical intersection in polyenic systems has been classified as a case A situation,[23,24] in which the CASSCF MXS determinations are considered accurate because the contribution of the differential correlation energy effects in both states is similar. The introduction of dynamical correlation by means of CASPT2 or MRCI methods is not expected to change the geometries in a large extent. Unfortunately this is not always the case as mentioned in previous sections. To determine crossing seams and MXS points in case B situations require dynamical correlation with methods more realistic than MRCI.[23,25] Regarding CASPT2, active spaces in larger molecular systems cannot be extended enough to make the off-diagonal elements less than 2 kcal/mol and the validation of the CASPT2 obtained results may be simply unpractical. On the other hand, MS-CASPT2 results calculated with small active spaces might yield unphysical avoiding crossings. The reliability of the results has to be determined in each case.

IV. CONCLUSIONS

Calculation of crossing seams and minimal-energy conical intersections responsible for the nonadiabatic photochemical processes in polyatomic systems of chemical and biological interest require in general efficient algorithms, as well as accurate and flexible quantum chemical methods able to include dynamic correlation effects. The currently and widely employed CASSCF procedure only works in those cases in which the differential dynamic correlation effects are negligible for the region of the hypersurfaces under consideration. Otherwise, procedures such as MRCI or CASPT2 seem unavoidable to obtain accurate results. Perturbative approaches such as CASPT2 are less expensive and more realistic in medium to large systems, and it would be desirable to find a straightforward application to compute state crossings. The single-state CASPT2 method yields however nonorthogonal wave functions, which clearly prevents its use in the calculation of degenerate points such a conical intersection. The multistate extension of the method, MS-CASPT2, can be suggested as a solution, considering that, in essence, it corresponds to an orthogonalization procedure of the CASPT2 solutions. We have reported in this paper a number of examples illustrating the behavior of both procedures, comparing to CASSCF and MRCI results when available.

The neutral-ionic avoided crossing between the two lowest $^1\Sigma^+$ states of the LiF molecule has been computed at both CASPT2 and MS-CASPT2 levels employing different active spaces. It is shown that, for small active spaces, while the CASPT2 curves lead to unphysical overlapped solutions, the application of the MS-CASPT2 orthogonalization is also incorrect at that level, yielding artificially large energy splittings in which the CASPT2 and the MS-CASPT2 state energies differ drastically. The same conclusion is basically

obtained when studying the conical intersection between the $1\,^1A_g/2\,^1A_g$ states in the ethene dimer and the S_0/S_1 states in the penta-2,4-dieniminium cation. The reason behind this discrepancy is that the CASPT2 results are poor references for the multistate procedure, and the coupling between them is too large. The off-diagonal elements of the MS-CASPT2 procedure are traced in the calculations showing the origin of the splitting. It is not until the reference is improved by enlarging the active spaces that the interaction decreases and the CASPT2/MS-CASPT2 treatment becomes similar. The convergence observed by increasing the active space is quite slow and in most cases consists of including angular correlation effects. Overall, the comparison with the MRCI MXS points in formaldehyde and the ethene dimer is good. The small discrepancies found in the obtained structures can be attributed either to the absence of the NACMEs in the CASPT2 determinations or to the known deficiencies of truncated MRCI procedures, usually yielding too high excitation energies. The similar geometries found in the CASSCF MXS determinations, both with and without NACMEs, points to the truncation carried out at the MRCI level as the main reason.

Equivalence in the CASPT2/MS-CASPT2 treatment is essential when computing state crossings because at a conical intersection the wave functions must be orthogonal. The example of formaldehyde and its $2\,^1A_1/1\,^1B_1$ conical intersection proves that CASPT2 can be safely used in that case because the states are orthogonal just by symmetry, as it would happen when computing crossings between states of different multiplicity. In other cases, CASPT2 can be used to compute energy differences, and MS-CASPT2 can be therefore added as a control of the accuracy of the determination. The present results suggest that if both solutions differ by less than certain energy difference, 1–2 kcal/mol, the results can be considered accurate and the computed energy difference may represent the crossing region properly. A CASPT2 energy difference between two states smaller than 2 kcal/mol can be considered a conical intersection, otherwise it represents an avoided crossing. Indeed, the lowest-energy solution leads us to the minimal of the crossing seam at this level of calculation. Unfortunately, this practical procedure cannot be applied to many molecules because of the technical limitations upon the increasing of the active space. Further methodological developments will be required if we want to extend the size of the problems under consideration.

For true conical intersections in a variational calculation, a nonzero difference in the energy of two surfaces can be considered a reflection of a geometric displacement away from the crossing seam. However, in determination of CIs by perturbation techniques the geometrical displacement is strongly coupled to the possible unphysical behavior of the methodology related mainly with the nonorthogonality of the wave functions involved. Once the correct perturbation treatment becomes operative (that is, leading to similar CASPT2 and MS-CASPT2 energy gaps), geometrical displacements from the seam occurring for energy differences smaller than 1–2 kcal/mol, are, in the molecules considered, really minor as it happens in a variational calculation.

ACKNOWLEDGMENTS

The research reported was supported by Project Nos. BQU2001-2926 and CTQ2004-01739 of the Spanish MCyT and MEC, and by Project No. GV04B-228 of the Generalitat Valenciana. The authors acknowledge helpful comments from Dr. P.-Å. Malmqvist.

[1] M. A. Robb, M. Olivucci, and F. Bernardi, in *Encyclopedia of Computational Chemistry*, edited by P. V. R. Schlegel *et al.* (Wiley, Chichester, 1998).
[2] D. R. Yarkony, in *Modern Electronic Structure Theory, Part I*, edited by D. R. Yarkony (World Scientific, Singapore, 1995).
[3] G. J. Atchity, S. S. Xantheas, and K. Ruedenberg, J. Chem. Phys. **95**, 1862 (1991).
[4] D. R. Yarkony, J. Chem. Phys. **114**, 2601 (2001).
[5] M. Klessinger and J. Michl, *Excited States and Photochemistry of Organic Molecules* (VCH, New York, 1995).
[6] H. Köppel, W. Domcke, and L. S. Cederbaum, Adv. Chem. Phys. **57**, 59 (1984).
[7] H. Lischka, M. Dallos, P. G. Szalay, D. R. Yarkony, and R. Shepard, J. Chem. Phys. **120**, 7322 (2004).
[8] N. Koga and K. Morokuma, Chem. Phys. Lett. **119**, 371 (1985).
[9] D. R. Yarkony, J. Phys. Chem. A **108**, 3200 (2004).
[10] A. Migani, M. A. Robb, and M. Olivucci, J. Am. Chem. Soc. **125**, 2804 (2003).
[11] L. De Vico, M. Olivucci, and R. Lindh (unpublished).
[12] B. O. Roos, P. R. Taylor, and P. E. M. Siegbahn, Chem. Phys. **48**, 157 (1980).
[13] B. O. Roos, Adv. Chem. Phys. **69**, 399 (1987).
[14] A. Farazdel and M. Dupuis, J. Comput. Chem. **12**, 276 (1991).
[15] D. R. Yarkony, J. Phys. Chem. **97**, 4407 (1993).
[16] M. R. Manaa and D. R. Yarkony, J. Chem. Phys. **99**, 5251 (1993).
[17] J. M. Anglada and J. M. Bofill, J. Comput. Chem. **18**, 992 (1997).
[18] I. N. Ragazos, M. A. Robb, F. Bernardi, and M. Olivucci, Chem. Phys. Lett. **197**, 217 (1992).
[19] M. J. Bearpark, M. A. Robb, and H. B. Schlegel, Chem. Phys. Lett. **223**, 269 (1994).
[20] B. O. Roos, P. Linse, P. E. M. Siegbahn, and M. R. A. Blomberg, Chem. Phys. **66**, 197 (1982).
[21] K. Andersson, P. Å. Malmqvist, B. O. Roos, A. J. Sadlej, and K. Wolinski, J. Phys. Chem. **94**, 5483 (1990).
[22] K. Andersson, P. Å. Malmqvist, and B. O. Roos, J. Chem. Phys. **96**, 1218 (1992).
[23] L. Serrano-Andrés and M. Merchán, in *Encyclopedia of Computational Chemistry*, edited by P. V. R. Schlegel *et al.* (Wiley, Chichester, 2004).
[24] M. Merchán and L. Serrano-Andrés, in *Computational Photochemistry*, edited by M. Olivucci (Elsevier, Amsterdam, 2005).
[25] M. Merchán and L. Serrano-Andrés, J. Am. Chem. Soc. **125**, 8108 (2003).
[26] S. S. Han and D. S. Yarkony, J. Chem. Phys. **119**, 11561 (2003).
[27] B. O. Roos, M. P. Fülscher, P.-Å Malmqvist, M. Merchán, and L. Serrano-Andrés, in *Quantum Mechanical Electronic Structure Calculations with Chemical Accuracy*, edited by S. R. Langhoff (Kluwer, Dordrecht, 1995).
[28] B. O. Roos, K. Andersson, M. P. Fülscher, P. Å. Malmqvist, L. Serrano-Andrés, K. Pierloot, and M. Merchán, Adv. Chem. Phys. **93**, 219 (1996).
[29] L. Serrano-Andrés, M. Merchán, I. Nebot-Gil, R. Lindh, and B. O. Roos, J. Chem. Phys. **98**, 3151 (1993).
[30] M. Merchán, L. Serrano-Andrés, M. P. Fülscher, and B. O. Roos, in *Recent Advances in Multireference Methods*, edited by K. Hirao (World Scientific, Singapore, 1999).
[31] C. S. Page and M. Olivucci, J. Comput. Chem. **24**, 298 (2003).
[32] J. Finley, P.-Å. Malmqvist, B. O. Roos, and L. Serrano-Andrés, Chem. Phys. **288**, 299 (1998).
[33] B. O. Roos, *A Perturbation-Variation Treatment of the Multi-State Problem in CASPT2* (Lund University, Lund, 1996).
[34] L. Serrano-Andrés, M. Merchán, and M. Jablonski, J. Chem. Phys. **119**, 4294 (2003).
[35] O. Rubio-Pons, L. Serrano-Andrés, and M. Merchán, J. Phys. Chem. A **105**, 9664 (2001).
[36] P. Celani and H.-J. Werner, J. Chem. Phys. **119**, 5044 (2003).
[37] K. Andersson, M. Barysz, A. Bernhardsson, *et al.*, MOLCAS 6.0, Department of Theoretical Chemistry, Chemical Centre, University of Lund, P.O.B. 124, S-221 000 Lund, Sweden, 2004.

[38]G. Karlström, R. Lindh, P.-Å. Malmqvist, *et al.*, Comput. Mater. Sci. **28**, 222 (2003).
[39]V. Veryazov, P.-O. Widmark, L. Serrano-Andrés, R. Lindh, and B. O. Roos, Int. J. Quantum Chem. **100**, 626 (2004).
[40]C. W. Bauschlicher, Jr., and S. R. Langhoff, J. Chem. Phys. **89**, 4246 (1988).
[41]J.-P. Malrieu, J.-L. Heully, and A. Zaitsevskii, Theor. Chim. Acta **90**, 167 (1995).
[42]C. Sousa, D. Domínguez-Ariza, C. de Graaf, and F. Illas, J. Chem. Phys. **113**, 9940 (2000).
[43]P.-O. Widmark, P.-Å. Malmqvist, and B. O. Roos, Theor. Chim. Acta **77**, 291 (1990).
[44]M. Dallos, H. Lischka, R. Shepard, D. R. Yarkony, and P. G. Szalay, J. Chem. Phys. **120**, 7330 (2004).
[45]T. H. Dunning, Jr., J. Chem. Phys. **90**, 1007 (1989).
[46]S. Matsika, J. Phys. Chem. A **108**, 7584 (2004).
[47]L. De Vico, C. S. Page, M. Garavelli, F. Bernardi, R. Basosi, and M. Olivucci, J. Am. Chem. Soc. **124**, 4124 (2002).